POLITECNICO DI TORINO
Repository ISTITUZIONALE

Design and validation of an innovative soft-sensor for pharmaceuticals freeze-drying monitoring

Original
Design and validation of an innovative soft-sensor for pharmaceuticals freeze-drying monitoring / Bosca, S., Fissore, D.. - In: CHEMICAL ENGINEERING SCIENCE. - ISSN 0009-2509. - STAMPA. - 66:21(2011), pp. 5127-5136. [10.1016/j.ces.2011.07.008]

Availability:
This version is available at: 11583/2428379 since: 2016-08-25T14:34:23Z

Publisher:
PERGAMON-ELSEVIER SCIENCE LTD

Published
DOI:10.1016/j.ces.2011.07.008

Terms of use:

This article is made available under terms and conditions as specified in the corresponding bibliographic description in the repository

Publisher copyright

(Article begins on next page)

28 November 2026

This is an electronic version (author's version) of the paper:

Bosca S., Fissore D. (2011). Design and validation of an innovative soft-sensor for pharmaceuticals freeze-drying monitoring. Chemical Engineering Science (Elsevier), 66(21), 5127-5136. DOI: 10.1016/j.ces.2011.07.008.

Design and validation of an innovative soft-sensor for pharmaceuticals freeze-drying monitoring

Serena Bosca, Davide Fissore[1]

Dipartimento di Scienza dei Materiali e Ingegneria Chimica,
Politecnico di Torino, corso Duca degli Abruzzi 24, 10129 Torino (Italy)

[1] Corresponding author
E-mail: davide.fissore@polito.it
Tel: +39-(0)11-0904693
Fax: +39-(0)11-0904699

Abstract

The paper is focused on the development of a Kalman filter type observer for the monitoring of the primary drying phase of the freeze-drying of pharmaceutical products in vials. The proposed soft-sensor is able to estimate the evolution of temperature of the product, the duration of the primary drying phase, the value of the overall heat transfer coefficient between the heating shelf and the product, as well as the mass transfer resistance of the dried cake to vapor flow. Accurate results are obtained for various types of products, characterized by a different dependence of the mass transfer resistance on the dried cake thickness. Theoretical results are confirmed by experimental tests carried out in a pilot-scale freeze-dryer. Finally, the strength and the weakness of the proposed observer are pointed out.

Key words

Drying; Product processing; Simulation; Bioprocessing; Freeze-drying; Soft-sensor; Monitoring; Extended Kalman Filter.

1. Introduction

Lyophilization is a drying process based on the sublimation of the solvent contained in the product to be treated. It is characterized by low operating temperatures and it is particularly suitable for those products, such as pharmaceuticals, which could be damaged by high temperature drying. Furthermore, the process allows obtaining a product with a porous structure that can be easily rehydrated and that can completely recover its properties after rehydration (see, among the others, Nail and Gatlin, 1992; Oetjen and Haseley, 2004; Franks, 2007).

The lyophilization process is carried out in three successive steps: freezing, primary drying, secondary drying. The most important phase is primary drying, when the vapor flows through the dried layer into the sublimation chamber, and then is continuously removed by a condenser. During this phase, process monitoring is crucial in order to obtain a product having the desired quality. In fact, it is required to monitor product temperature because it has to be maintained below a limit value. In the case of crystalline solutes, this limit temperature corresponds to the eutectic point, in order to avoid the formation of a liquid phase; if the solutes are amorphous, the limit value is the glass transition temperature in order to avoid the collapse of the dried cake.

Another important variable that is useful to monitor is the position of the sublimation interface, whose evolution is representative of the progress of primary drying. This variable allows to know when it is possible to increase the set-point of the temperature of the heating fluid in order to allow the desorption of the water bounded to the product (secondary drying). If the secondary drying is started too early, the temperature of the product is increased when sublimation is still occurring, thus causing the melting of the ice and damaging the product. If secondary drying is delayed, the length and cost of the process are increased.

The use of an effective in-line monitoring system allows closing a control loop, thus manipulating the operating conditions, namely shelf temperature and chamber pressure, in order to preserve (and also to build) product quality during processing (Fissore et al., 2008). This is one of the targets indicated by the Guidance for Industry PAT (Process Analytical Technology), issued by US-FDA in 2004: quality has no longer to be tested into products, but it has to be built-in or it should be by design

In order to monitor the freeze-drying process it is possible to use a soft-sensor (observer), i.e. a device that uses a mathematical model of the process and the experimental measurements of one or more physical variables to provide an in-line estimation of the

product state and of other variables of interest. Various techniques were proposed in the literature to design an observer, e.g. the Extended Kalman Filter and the High Gain Technique. Velardi et al. (2009) proposed to use the Extended Kalman Filter to monitor the primary drying phase of a freeze-drying process: they used the measurement of the temperature of the product at the bottom of the vial, obtained inserting a thermocouple in the vial, and a simple mono-dimensional model of the process (Velardi and Barresi, 2008) to estimate in-line the temperature of the product, the position of the sublimating interface, the mass transfer resistance to vapor flow and the heat transfer coefficient. Velardi et al. (2010) designed also a High Gain observer to monitor the primary drying of a lyophilization process, evidencing that the accuracy of the estimations is similar to that obtained using the Extended Kalman Filter, but the time required by the calculations is significantly reduced, even if it is required to manipulate the system of differential equations modeling the dynamics of the system in order to get a structure suitable for the design of the High Gain observer. Both the Extended Kalman filter and the High Gain observer were developed for a particular type of product, characterized by a linear dependence of the mass transfer resistance (R_p) on the dried layer thickness (H); thus, these tool are only suitable for that type of product and they can not be used to monitor those products characterized by a non-linear dependence of R_p on H. Actually, the majority of products dried by means of a lyophilization process is characterized by a non linear dependence of R_p on H: this motivates the need for a new observer that is able to monitor all types of products. The Extended Kalman Filter approach will be chosen to built the desired observer, as the process is highly non-linear.

The paper is structured as follows: at first, the structure of the proposed observer is introduced and, then, it will be validated by means of numerical and experimental investigations. The numerical validation is carried out to verify that the estimations provided by the observer converges to the true values (as in this case the state of the product is fully known from mathematical simulation), while the experimental validation is carried out to prove the adequacy of the soft-sensor to monitor real lyophilization cycles.

2. Non-linear observer design

The Kalman filter was firstly proposed by Rudolph E. Kalman in 1960 as a solution for the linear discrete data filtering problem (Kalman, 1960): it is a set of equations implementing a predictor-corrector estimator that minimizes the covariance of the estimation error. The filter

was developed for a discrete-time system, but it has also been applied to continuous-time systems, as well as to non-linear processes (Becerra et al., 2001; Judd, 2003).

Let us consider the dynamics of a system described by the following set of differential equations:

$$\dot{\mathbf{x}} = \mathbf{f}\left(\mathbf{x}, u\right) \tag{1}$$

where **x** is the array of state variables, u is the manipulated input and **f** is a non-linear function of **x** and u. Let y be the measured variable:

$$y = h\left(\mathbf{x}, u\right) \tag{2}$$

The Kalman filter type observer for the system described by equations (1)-(2) is based on the following equations:

$$\dot{\hat{\mathbf{x}}} = \mathbf{f}\left(\hat{\mathbf{x}}, u\right) + \mathbf{K}\left(t\right)\left(\hat{y} - y\right) \tag{3}$$

$$\hat{y} = \mathrm{h}\left(\hat{\mathbf{x}}, u\right) \tag{4}$$

$$\mathbf{K}\left(t\right) = \mathbf{S}^{-1}\left(t\right)\left(\left.\frac{\partial h}{\partial \mathbf{x}}\right|_{\hat{x}}\right)^{T} \tag{5}$$

$$\dot{\mathbf{S}}\left(t\right) = -\left(\left.\frac{\partial \mathbf{f}}{\partial \mathbf{x}}\right|_{\hat{\mathbf{x}}}\right)^{T}\mathbf{S}\left(t\right) - \mathbf{S}\left(t\right)\left.\frac{\partial \mathbf{f}}{\partial \mathbf{x}}\right|_{\hat{\mathbf{x}}} + \left(\left.\frac{\partial h}{\partial \mathbf{x}}\right|_{\hat{\mathbf{x}}}\right)^{T}\left.\frac{\partial h}{\partial \mathbf{x}}\right|_{\hat{\mathbf{x}}} - \mathbf{S}\left(t\right)\Lambda\mathbf{S}\left(t\right) \tag{6}$$

A detailed derivation of equations (3)-(6) can be found in various papers, e.g. in the Appendix A of the paper by Velardi et al. (2009). It has to be remarked that these equations have been obtained after a linearization of model equations (1)-(2) and, thus, the estimations of the state variables provided by the observer ($\hat{\mathbf{x}}$) are guaranteed to converge to the real values (**x**) only in case the approximation introduced by the linearization is small. This makes the first guess of the estimated variables a critical step.

The equations of the observer are based on the mathematical model of the process. For a vial freeze-drying process various models have been proposed to describe the evolution of the temperature of the product and of the amount of ice *vs*. time as a function of the operating conditions (a brief review can be found in Velardi and Barresi, 2008). In this paper we use the simplified mono-dimensional model of Velardi and Barresi (2008): according to this model, the heat flux to the product and the solvent sublimation flux are calculated using the following equations:

$$J_q = K_v\left(T_{fluid} - T_B\right) \tag{7}$$

$$J_w = \frac{1}{R_p}\left(p_{w,i} - p_{w,c}\right) \tag{8}$$

K_v is the overall heat transfer coefficient between the heating fluid and the product at the bottom of the vial and R_p is the resistance of the dried product to vapor flow. The coefficient K_v is a function of chamber pressure, for a given vial-freeze-dryer system:

$$K_v = a_{K_v} + \frac{b_{K_v} p_c}{1 + c_{K_v} p_c} \tag{9}$$

while R_p is a function of the thickness of the dried layer (H), for a given product. The following equation is generally proposed to describe the dependence of R_p on H:

$$R_p = R_{p,0} + \frac{A_{R_p} \cdot H}{1 + B_{R_p} \cdot H} \tag{10}$$

where $R_{p,0}$, A_{R_p}, B_{R_p} depend on the product under investigation. In case $R_{p,0} \to 0$ and $B_{R_p} \to 0$, the dependence of R_p on H is linear:

$$R_p = A_{R_p} \cdot H \tag{11}$$

as in the model used by Velardi et al. (2009, 2010) to design a soft-sensor for the vial freeze-drying process, where:

$$R_p = \left(\frac{R \cdot T_i}{M \cdot k_1} \right) \cdot H \tag{12}$$

At the moving interface there is no heat accumulation, and the heat flux is used for ice sublimation:

$$\left(\frac{1}{K_v} + \frac{L - H}{k_{II}} \right)^{-1} \left(T_{fluid} - T_i \right) = \Delta H_S \frac{1}{R_p} \left(p_{w,i} - p_{w,c} \right) \tag{13}$$

The following equation gives product temperature at the vial bottom:

$$T_B = T_{fluid} - \frac{1}{K_v} \left(\frac{1}{K_v} + \frac{L - H}{k_{II}} \right)^{-1} \left(T_{fluid} - T_i \right) \tag{14}$$

Finally, the evolution of frozen product thickness is calculated by solving the following equation:

$$\frac{dH}{dt} = -\frac{1}{\rho_{II} - \rho_{Ie}} \frac{1}{R_p} \left(p_{w,i} - p_{w,c} \right) \tag{15}$$

This model has been extensively validated by means of experiments (see, among the others, Velardi and Barresi, 2008, and Giordano et al., 2011).

Various methods have been proposed to calculate model parameters (K_v and R_p). The coefficients a_{K_v}, b_{K_v} and c_{K_v} can be calculated through various theoretical expressions

provided in the literature (see, among the others, Pikal et al., 1984); in any case experimental investigation is necessary to determine these values reliably. To this purpose a gravimetric method can be used. It requires to carry out a lyophilization cycle under well defined operating conditions (temperature and pressure) and filling the vials of the batch with water (or a solution). The ice temperature at the bottom of the vial (T_B) and the weight loss of water (Δm) in each vial have to be measured. The value of K_v can be calculated using the following equation:

$$K_v = \frac{\Delta m \cdot \Delta H_s}{\Delta t \cdot \left(T_{shelf} - T_B\right) \cdot A_v} \tag{16}$$

As an alternative, the value of the sublimation flux ($\Delta m / \left(\Delta t \cdot A_v\right)$) required to calculate K_v can be determined using the Tunable Diode Laser Absorption Spectroscopy (Kessler et al., 2006; Gieseler et al., 2007; Kuu et al., 2009). Another method to obtain the value of K_v is based on the use of the algorithms proposed for the monitoring of the primary drying using the pressure rise test (Milton et al., 1997; Chouvenc et al., 2004; Velardi et al., 2008; Fissore et al., 2011). In any case, at least three measurements at three different values of p_c, are required to determine the values of a_{K_v}, b_{K_v} and c_{K_v}.

The parameter R_P can be determined from the measurement of the solvent flux, obtained using the Tunable Diode Laser Absorption Spectroscopy sensor, as shown in the following equation:

$$R_p = \frac{p_{w,i} - p_c}{J_w} \tag{17}$$

or one of the algorithms used to interpret the pressure rise test. Furthermore, Fissore et al. (2010) proposed to use a special device placed in the lyophilization chamber to calculate R_p using of the measurement of the weight loss due to the sublimation of ice *vs.* time (i.e. of J_w) and of product temperature in the weighed vials (used to calculate $p_{w,i}$).

For the process under investigation the state vector that the soft sensor has to estimate is the following:

$$\mathbf{x} = \begin{pmatrix} x_1 & x_2 & x_3 \end{pmatrix}^T = \begin{pmatrix} T_{\mathrm{i}} & A_{R_p} & K_v \end{pmatrix}^T \tag{18}$$

It can be remarked that the parameter A_{R_p} has been selected to account for the value of R_p (the values of $R_{p,0}$ and B_{R_p} have been kept constant and equal to their first estimations) thus reducing the number of variables that the soft-sensor has to estimate. The measured variable of the process (y) is the product temperature at the bottom of the vial. The manipulated

variable (u) is the temperature of the heating fluid. Model equation can then be written as in equations (1) and (2):

$$\begin{cases} \dot{\mathbf{x}} = \mathbf{f}\left(\mathbf{x},u\right) = \begin{pmatrix} \dot{x}_1 \\ \dot{x}_2 \\ \dot{x}_3 \end{pmatrix} = \begin{pmatrix} f_1\left(x_1,x_2,x_3,u\right) \\ 0 \\ 0 \end{pmatrix} \\ y = \mathbf{h}\left(\mathbf{x},u\right) = h\left(x_1,x_2,x_3,u\right) \end{cases} \tag{19}$$

where the first derivative of x_2 and x_3 are set equal to zero because the parameters A_{R_p} and K_v do not change during the freeze-drying process. The following equation is used to calculate the first derivative of $x_1 = T_i$ with respect to time:

$$\frac{dx_1}{dt} = \left(\frac{dH}{dt} - \frac{\partial H}{\partial u}\frac{du}{dt}\right)\left(\frac{\partial H}{\partial x_1}\right)^{-1} \tag{20}$$

Equation (20) requires the partial derivatives of H with respect to x_1, u and t. To this purpose, it is necessary to determine the dependence of H on the state variables. By means of simple manipulations of equation (14) we get:

$$H = \frac{\alpha - \beta}{\frac{\beta}{R_{p,0}}\gamma - \alpha B_{R_p}} \tag{21}$$

where:

$$\alpha = \alpha\left(x_1,x_3\right) = \frac{\Delta H_s}{x_3}\left(p_{w,i}\left(x_1\right) - p_{w,c}\right) \tag{22}$$

$$\beta = \beta\left(x_1,u\right) = R_{p,0}\left(u - x_1\right) \tag{23}$$

$$\gamma = \gamma\left(x_2\right) = R_{p,0}B_{R_p} + x_2 \tag{24}$$

Using equations (21)-(24) we calculate:

$$\frac{dH}{dt} = \frac{x_3\left(\frac{\gamma}{R_{p,0}} - B_{R_p}\right)\beta}{\delta\left(\gamma - R_{p,0}B_{R_p}\right)} \tag{25}$$

$$\frac{\partial H}{\partial x_1} = \frac{\left(\frac{\gamma}{R_{p,0}} - B_{R_p}\right)}{\left(\frac{\gamma}{R_{p,0}}\beta - \alpha B_{R_p}\right)^2}\left(\beta\frac{\partial\alpha}{\partial x_1} - \alpha\frac{\partial\beta}{\partial x_1}\right) \tag{26}$$

where

$$\delta = \Delta H_S \cdot \left(\varrho_{II} - \varrho_{Ie}\right) \tag{27}$$

At first we assume that $\frac{du}{dt}=0$ and, thus, the calculation of $\frac{\partial H}{\partial u}$ is not necessary: this assumption is justified by the fact that in most freeze-drying processes the shelf temperature is maintained constant throughout primary drying. Furthermore, this assumption allows to simplify the equations of the observer, and it can be useful also for validation purposes because the degrees of freedom of the system are reduced. In case $\frac{du}{dt}\neq 0$ subsequent equations are modified and they are shown in Appendix A. When $\frac{du}{dt}=0$, equation (20) becomes:

$$\frac{dx_1}{dt}=\frac{dH}{dt}\left(\frac{\partial H}{\partial x_1}\right)^{-1} \tag{28}$$

By combining equations (25) and (26) into equation (28), and expressing the measured variable as a function of the state variables, we get:

$$\begin{cases}\dot{\mathbf{x}}=\begin{pmatrix}\dfrac{1}{\delta}\dfrac{x_3\left(\dfrac{\gamma}{R_{P,0}}\beta-\alpha B_{R_p}\right)^2\beta}{\left(\gamma-R_{p,0}B_{R_p}\right)\left(\beta\dfrac{\partial\alpha}{\partial x_1}-\alpha\dfrac{\partial\beta}{\partial x_1}\right)}\\0\\0\end{pmatrix}=\mathbf{f}\left(\mathbf{x},u\right)\\ y=u-\dfrac{\beta}{R_{p,0}}=\mathbf{h}\left(\mathbf{x},u\right)\end{cases} \tag{29}$$

In order to calculate the gain of the observer $\mathbf{K}(t)$ we need the Jacobian matrix $\partial\mathbf{f}/\partial\mathbf{x}$ and the vector $\partial\mathbf{h}/\partial\mathbf{x}$:

$$\left.\frac{\partial\mathbf{f}}{\partial\mathbf{x}}\right|_{\hat{\mathbf{x}}}=\begin{bmatrix}\dfrac{\partial f_1}{\partial x_1} & \dfrac{\partial f_1}{\partial x_2} & \dfrac{\partial f_1}{\partial x_3}\\0 & 0 & 0\\0 & 0 & 0\end{bmatrix}_{\hat{\mathbf{x}}} \tag{30}$$

$$\left.\frac{\partial\mathbf{h}}{\partial\mathbf{x}}\right|_{\hat{\mathbf{x}}}=\begin{pmatrix}\dfrac{\partial h}{\partial x_1} & \dfrac{\partial h}{\partial x_2} & \dfrac{\partial h}{\partial x_3}\end{pmatrix}_{\hat{\mathbf{x}}} \tag{31}$$

The components of $\partial\mathbf{f}/\partial\mathbf{x}$ and of $\partial\mathbf{h}/\partial\mathbf{x}$ are obtained from the equations (29):

$$\frac{\partial f_1}{\partial x_1}=\frac{1}{\delta}\frac{x_3\dfrac{\partial\beta}{\partial x_1}\left(\dfrac{\gamma}{R_{p,0}}\beta-\alpha B_{R_p}\right)^2+2x_3\beta\left(\dfrac{\gamma}{R_{p,0}}\beta-\alpha B_{R_p}\right)\left(\dfrac{\gamma}{R_{p,0}}\dfrac{\partial\beta}{\partial x_1}-B_{R_p}\dfrac{\partial\alpha}{\partial x_1}\right)}{\left(\gamma-R_{p,0}B_{R_p}\right)\left(\beta\dfrac{\partial\alpha}{\partial x_1}-\alpha\dfrac{\partial\beta}{\partial x_1}\right)}+$$
$$+\frac{1}{\delta}\frac{x_3\beta\left(\dfrac{\gamma}{R_{p,0}}\beta-\alpha B_{R_p}\right)^2}{\left(\gamma-R_{p,0}B_{R_p}\right)}\frac{\alpha\dfrac{\partial^2\beta}{\partial x_1^{\,2}}-\beta\dfrac{\partial^2\alpha}{\partial x_1^{\,2}}}{\left(\beta\dfrac{\partial\alpha}{\partial x_1}-\alpha\dfrac{\partial\beta}{\partial x_1}\right)^2} \tag{32}$$

$$\frac{\partial f_1}{\partial x_2}=\frac{1}{\delta}\frac{x_3}{\alpha\dfrac{\partial\beta}{\partial x_1}-\beta\dfrac{\partial\alpha}{\partial x_1}}\frac{\partial\gamma}{\partial x_2}\frac{2\dfrac{\beta^2}{R_{p,0}}\left(\dfrac{\gamma}{R_{p,0}}\beta-\alpha B_{R_p}\right)\left(\gamma-R_{p,0}B_{R_p}\right)-\beta\left(\dfrac{\gamma}{R_{p,0}}\beta-\alpha B_{R_p}\right)^2}{\left(\gamma-R_{p,0}B_{R_p}\right)^2} \tag{33}$$

$$\frac{\partial f_1}{\partial x_3}=\frac{1}{\delta}\frac{\beta\left(\dfrac{\gamma}{R_{p,0}}\beta-\alpha B_{R_p}\right)^2-2x_3\beta\left(\dfrac{\gamma}{R_{p,0}}\beta-\alpha B_{R_p}\right)\dfrac{\partial\alpha}{\partial x_3}B_{R_p}}{\left(\gamma-R_{p,0}B_{R_p}\right)\left(\beta\dfrac{\partial\alpha}{\partial x_1}-\alpha\dfrac{\partial\beta}{\partial x_1}\right)}+$$
$$+\frac{1}{\delta}\frac{x_3\beta\left(\dfrac{\gamma}{R_{p,0}}\beta-\alpha B_{R_p}\right)^2}{\left(\gamma-R_{p,0}B_{R_p}\right)}\frac{\left(\dfrac{\partial\beta}{\partial x_1}\dfrac{\partial\alpha}{\partial x_3}-\beta\dfrac{\partial^2\alpha}{\partial x_1\partial x_3}\right)}{\left(\beta\dfrac{\partial\alpha}{\partial x_1}-\alpha\dfrac{\partial\beta}{\partial x_1}\right)^2} \tag{34}$$

$$\frac{\partial h}{\partial x_1}=-\frac{1}{R_{p,0}}\frac{\partial\beta}{\partial x_1} \tag{35}$$

$$\frac{\partial h}{\partial x_2}=\frac{\partial h}{\partial x_3}=0 \tag{36}$$

Finally, it is necessary to calculate the derivative of the functions $\alpha(x_1,x_3)$, $\beta(x_1,u)$, $\gamma(x_2)$, that can be determined from equations (22)-(24):

$$\frac{\partial\alpha}{\partial x_1}=\frac{\Delta H_s}{x_3}\frac{dp_{w,i}}{dx_1} \tag{37}$$

$$\frac{\partial^2\alpha}{\partial x_1^2}=\frac{\Delta H_S}{x_3}\frac{d^2p_{w,i}}{dx_1^2} \tag{38}$$

$$\frac{\partial\alpha}{\partial x_3}=-\frac{\Delta H_S}{x_3^2}\left(p_{w,i}-p_c\right) \tag{39}$$

$$\frac{\partial \alpha}{\partial x_1 \partial x_3} = -\frac{\Delta H_s}{x_3^2}\frac{dp_{w,i}}{dx_1^2} = -\frac{1}{x_3}\frac{\partial \alpha}{\partial x_3} \tag{40}$$

$$\frac{\partial \beta}{\partial x_1} = -R_{p,0} \tag{41}$$

$$\frac{\partial^2 \beta}{\partial x_1^2} = 0 \tag{42}$$

$$\frac{\partial \gamma}{\partial x_2} = 1 \tag{43}$$

3. Case studies

The validation of the observer is carried out in two steps. In the first phase, process simulation using the model of Velardi and Barresi (2008) has been used to calculate the evolution of a product characterized by a non-linear dependence of the resistance R_p on dry cake thickness, as described by equation (10), and, thus, the temperature of the product at the bottom of the vial required by the observer. By this way it is possible to compare the estimations of interface product temperature, frozen layer thickness, and model parameters with the true values, thus validating the tool. Two different case studies have been considered to this purpose: in the first case the product is characterized by a high value of resistance to vapor flow (i.e. of A_{R_p}) and a high value of K_v; in the second case we considered lower values of A_{R_p} and K_v. By this way we are able to account for the large variability of A_{R_p} and K_v when processing different products and, consequently, we are able to test the effectiveness of the soft sensor in case the process is heat-transfer controlled, as well as when freeze-drying is mass-transfer controlled.

Afterwards, the performance of the observer used to monitor the dynamics of a product characterized by a linear dependence of resistance R_p on dry cake thickness, as shown in equation (12), has been investigated, in order to demonstrate the possibility of applying the proposed observer to a wide variety of products. Also in this case the values of the temperature at the bottom of the vial obtained by mathematical simulation are provided to the observer, and the convergence of the proposed tool is verified.

Finally, experimental investigation has been used to verify the adequacy of the tool to monitor the primary drying phase of a real freeze-drying cycle. In this case a thermocouple

placed at the bottom of the vial is used to provide the product temperature measurement. The lyophilization cycle is carried out in a *LyoBeta* 25™ freeze-dryer (Telstar, Spain), using ISO 8362-1 10R tubing vials filled with 2.5 ml of a 10% w/w aqueous solution of an active pharmaceutical ingredient, corresponding to 7.6 mm of product thickness. In this case the temperature of the heating shelf was not constant, while chamber pressure was kept constant and equal to 5 Pa. Product temperature was measured using a T-type miniature thermocouple (by Tersid S.p.A., Milano, Italy). It has to be remarked that the evolution of the product in vials placed in various positions over the shelf can be different according to various heat transfer mechanisms affecting the thermal balance of the product (Barresi et al., 2010a, 2010b). With this respect, vials of the first rows receive additional heat due to radiation from chamber walls. Thus, for this test we have monitored the dynamics of product temperature in a vial placed in a central position over the shelf as it is representative of the largest part of the batch

4. Results and discussion

Numerical validation of the observer is carried out by using the mathematical model to simulate the primary drying. Figure 1 shows the results obtained for two different case studies, characterized by different values of K_v and A_{R_p}: in the first K_v = 30 J $s^{-1}m^{-2}K^{-1}$ and A_{R_p} = $1 \cdot 10^9$ s^{-1}, while in the second K_v = 10 J $s^{-1}m^{-2}K^{-1}$ and A_{R_p} = $2 \cdot 10^8$ s^{-1}. Both shelf temperature and chamber pressure have been considered constant throughout primary drying. In order to test the performance of the observer, the initial values of $\hat{K}_v$ and $\hat{A}_{R_p}$ have been set with an error of 5% compared to the reported true values. An excellent agreement is obtained between the temperature estimated by the observer and the true value; a good agreement is obtained with respect to the position of the moving interface vs. time, with an error on the estimation of the duration of primary drying of -1.6 % in the first case, and of -3.9 % in the second case. As far as model parameters are concerned, the error on the estimation of R_p remains very small (lower than 5%), while the estimated value of K_v moves from the wrong initial guess to the true value in both cases. This is of outmost importance as the observer is not only able to provide a reliable estimation of product temperature at the interface of sublimation and of the sublimation flux (i.e. of the position of the sublimating interface, and of the duration of the primary drying), but it provides also reliable values of

model parameters and, thus, it can be used in a model-based control loop (Fissore et al., 2008). In both cases we tested also the performance of the observer proposed by Velardi et al. (2009), evidencing that it does not converge to the correct values: as an example, the error on the duration of the primary drying is about 150%. These results confirm that the observer proposed by Velardi (2009) is able to monitor only the dynamics of those products that exhibit a linear dependence of the mass transfer resistance on the dried layer thickness.

As it has been pointed out in the Introduction section, the convergence of the Kalman filter is guaranteed only in case the initial values of the estimated variables are sufficiently close to the real values. For this purpose it is worthwhile to analyze the effect of the initial error on the state variables on the performance of the observer. For this study we have considered a product whose resistance R_P is calculated using the following parameters: $R_{p,0}$ = 11300 m s^{-1}, $A_{R_p} = 4.1 \cdot 10^8$ s^{-1} and $B_{R_p} = 1920$ m^{-1}; the value of the heat transfer coefficient is K_v = 17.1 J $s^{-1}m^{-2}K^{-1}$. The values of K_v and R_p considered in this study corresponds to those obtained experimentally for the 10% w/w aqueous solution of the drug considered at the end of this section as case study for the experimental validation of the observer. Chamber pressure is considered constant at 8 Pa, and the heating fluid temperature is equal to -10°C. Wrong values of the parameters K_v and A_{R_p} are provided to the observer at $t = 0$ in order to verify the ability of the observer to converge to the correct values, starting from a bad estimation; the values of $\hat{K}_v(t=0)$ and $\hat{A}_{R_p}(t=0)$ are summarized in Table 1. Figure 2 shows the observer predictions in all the cases. In Figure 2 (a), the evolution of product temperature is shown, thus evidencing that the observer is able to provide good estimates regardless of the initial error on the value of parameters. The same results are obtained when considering the evolution of the moving front, shown in Figure 2 (b), and this proves that the evaluation of the duration of the primary drying obtained using the observer is reliable in all the cases (the error ranges from -0.7 % in case 4 to -5 % in case 2). Finally, Figures 2 (c) and (d) show that also the parameters K_v and R_p are correctly estimated, despite their final values are not perfectly coincident with the true ones, used by the mathematical model. This fact can be explained by considering that the observer, during its calculations, minimizes the difference between the model estimated temperature and the calculated one, and it is possible to find various couples of values of the parameters resulting in the same value of temperature. This leads to the conclusion that the final values of K_v and R_p are the results of a compensation between the values of the same parameters. Furthermore, by observing the Figure 2 (c) and (d) it is

possible to underline that if initial guesses of K_v and R_p are both higher (or lower) than the true values, the tool is able to reduce the estimation error, otherwise the error can be increased.

With respect to the convergence of the observer calculations, it is interesting to investigate the maximum error allowed for the initial estimation of the parameters K_v and A_{R_p} to obtain the convergence of the observer. In this study we have considered that the initial value of product temperature is perfectly known, as it is generally the case when using a thermocouple to monitor product drying. The results of this study are presented in Figure 3, where the set of errors on $\hat{K}_v(t=0)$ and on $\hat{A}_{R_p}(t=0)$ that guarantee the convergence of the observer, is evidenced. More precisely we observe that the estimation error on the initial estimation of A_{R_p} can roughly vary between -5% and +10% compared to the true value, while the error on the initial estimation of K_v can vary between -25% and +25% compared to the true value. In those ranges of parameters values the observer provide correct estimations, i.e. an error on the duration of the primary drying lower than 5%, and a maximum error on product temperature lower than 0.5°C. The occurrence of a relevant error on the initial estimation of product temperature has also been investigated, evidencing that the convergence of the observer is not significantly affected by the initial error on product temperature. Results of Figure 3 are of outmost importance if we consider that, using the methods previously described (e.g. the gravimetric method for K_v or the pressure rise test for R_p) to determine the parameters K_v and A_{R_p}, their values are affected by uncertainty (generally about 5-10%). Thus, the observer is able to correct the initial estimation of model parameters in order to provide reliable estimations of the temperature at the interface of sublimation and of the sublimation flux (i.e. of the drying time), using the measurement of product temperature at the bottom of the container.

Figure 4 shows the results obtained when using the proposed observer to monitor the dynamics of a product whose dependence of the mass transfer resistance on the dry cake thickness is linear, as for the product considered by Velardi et al. (2009). In this case we considered the following parameters to calculate R_p: $R_{p,0}$ = 33969 m s^{-1}, A_{R_p} = $1.06 \cdot 10^8$ s^{-1} and B_{R_p} = 0 m^{-1}; the parameter K_v has been considered equal to 16.2 J $s^{-1}m^{-2}K^{-1}$. These parameter correspond to the values experimentally determined for a 5% w/w aqueous solution of lactose, processed in vials characterized by an internal diameter of 16.1 mm and a mean thickness of the vial bottom of 0.84 mm. As in the previous cases, chamber pressure and

heating fluid temperature have been considered constant and equal to 8 Pa and -10°C respectively. Also in this case the agreement between the correct values of product temperature, interface position, and model parameters with the values estimated by the soft-sensor is very good. It can be pointed out that the dependence of the estimated values of R_p vs. L_{dried} is not perfectly linear: this is due to the fact that the observer continuously estimates A_{R_p} during primary drying and, in this case, small variations in the estimated value of this parameter are responsible for the small variation in the slope of the curve of $\hat{R}_p$ vs. L_{dried}. Thus, we can conclude that the proposed observer can be applied to various type of products, and in all cases it provides a good estimation of the variables of interest.

Once the observer has been validated by means of numerical simulation, it is possible to prove its adequacy to monitor a real lyophilization cycle. The experimental validation is carried out with data obtained in freeze-drying cycles performed in laboratory and, as indicated in the previous section, the product that is freeze-dried is a 10% w/w aqueous solution of an active pharmaceutical ingredient. Preliminary investigation was required to determine the values of K_v and A_{R_p} for this system: the previously described gravimetric method was used to determine the overall heat transfer coefficient to the product, while the DPE algorithm (Velardi et al., 2008), proposed to interpret the pressure rise test, was used to determine A_{R_p}. Both values were adopted as the initial estimations of model parameters required by the observer. In order to test the robustness of the soft-sensor we considered also different values of $\hat{K}_v(t=0)$ and $\hat{A}_{R_p}(t=0)$, as shown in Table 2. The initial value of product temperature, in all the cases, has been considered equal to the first measure provided by the thermocouple at the bottom of the vial placed in a central position over the shelf. It has to be remarked that in this test the temperature of the heating shelf was not constant, and this is responsible of the evolution of product temperature that shows a maximum at about 1.5 h from the beginning of the primary drying. Although $du/dt \neq 0$, we used the observer designed assuming $du/dt = 0$ and a good agreement between the true and the estimated values of product temperature was obtained, as shown in Figure 5. The error in the estimation of the duration of primary drying ranges from -3% to 5%. This result is due to the fact that the convergence of the observer is very fast, and the rate of change of fluid temperature is quite slow, as in most freeze-drying processes. This allows to use the observer (21)-(43). Obviously, in case the rate of change of T_{fluid} is high, the observer given in Appendix A has to be used. Also in this case we have tested the robustness of the observer, looking for the

maximum errors on $\hat{K}_v(t=0)$ and $\hat{A}_{R_p}(t=0)$ that guarantee the convergence of the observer. Results are shown in Figure 6, evidencing that the set of values of errors on K_v and on A_{R_p} is similar to that shown in Figure 3 for the simulated experiment.

5. Conclusions.

A new observer for monitoring the primary drying phase of a lyophilization process has been designed in this paper. It is able to estimate reliably product temperature and the duration of primary drying, as well as model parameters describing heat transfer to the product and mass transfer from the interface of sublimation. The soft-sensor has been validated by means of numerical simulations and experimental tests, thus pointing out the strength of this tool, that is able to reliably monitor the dynamics of the temperature of the product and of the position of the interface of sublimation, and also to estimate the parameters of a simple model of the process, thus allowing the use of model-based control systems, as proposed by Fissore et al. (2008). Moreover, this soft-sensor appears to be quite robust with respect to the initial estimations of model parameters and of product temperature, and this is an important issue as the values of these parameters can be determined mainly with an experimental investigation and, thus, their values are affected by uncertainty. Moreover, using the proposed soft-sensor it is possible to monitor various vials placed in different positions in the freeze-dryer, thus allowing taking into account the heterogeneity of the batch due to the different heat transfer mechanisms to the product (e.g. radiation from chamber walls, or non-uniform temperature of the heating fluid). Finally, the soft-sensor has provided reliable estimations with various types of products, characterized by a different dependence of R_p on dried cake thickness, even in case the temperature of the heating fluid is not constant.

The main weakness related to the use of this sensor is due to the use of a thermocouple to get the temperature measurement. The use of wireless sensors recently proposed (Vallan et al., 2005; Corbellini et al., 2010) may allow the use of thermocouples with the automatic loading/unloading systems used in industrial freeze-dryers. Finally, the insertion of a thermocouple in the vial could not be allowed because of sterility reasons, or because the presence of the thermocouple can affect the dynamics of the product. In this case it could be possible to place the thermocouple on the external wall of the vial (Grassini et al., 2009), thus avoiding any interference with the product. An example of observer for a product exhibiting a

linear dependence of R_p on dried cake thickness and using the measurement of the temperature of the external wall was patented by Barresi et al. (2007).

Acknowledgements

Valuable suggestions of prof. A. Barresi (Politecnico di Torino) are gratefully acknowledged.

List of Symbols

a_{K_v}	parameter used to calculate K_v, J m^{-2}s^{-1}K^{-1}
A_{R_p}	parameter used to calculate R_p, s^{-1}
A_v	cross sectional area of the vial, m^2
b_{K_v}	parameter used to calculate K_v, J m^{-2}s^{-1}K^{-1}Pa^{-1}
B_{R_p}	parameter used to calculate R_p, m^{-1}
c_{K_v}	parameter used to calculate K_v, Pa^{-1}
e_{K_v}	error on the initial estimation of K_v, $\frac{\hat{K}_v(t=0)-K_v}{K_v}$
$e_{A_{R_p}}$	error on the initial estimation of A_{R_p}, $\frac{\hat{A}_{R_p}(t=0)-A_{R_p}}{\hat{A}_{R_p}}$
f	vectorial function giving the derivatives of the state
h	state space equation of the measured variable
H	moving front position (thickness of the dried layer), m
ΔH_s	enthalpy of sublimation, J kg^{-1}
J_q	heat flux, J m^{-2}s^{-1}
J_w	sublimation flux of water, kg m^{-2}s^{-1}
k_1	effective diffusivity coefficient, m^2 s^{-1}
k_{II}	thermal conductivity of the frozen layer, J m^{-1}s^{-1}K^{-1}
K	observer gain
K_v	overall heat transfer coefficient, W m^{-2}K^{-1}
L	total product thickness, m
Δm	weight loss of water, kg
M	water molecular weight, kg kmol^{-1}
p_c	chamber pressure, Pa
$p_{w,c}$	water partial pressure in the drying chamber, Pa
$p_{w,i}$	water pressure at the interface of sublimation, Pa
R	ideal gas constant, J mol^{-1} K^{-1}
R_p	mass transfer resistance, m s^{-1}
$R_{p,0}$	parameter used to calculate R_p, m s^{-1}
S	matrix used to calculate the observer gain

T_i	product temperature at the sublimation interface, K
T_B	temperature of the product at the bottom of the vial, K
T_{fluid}	heating fluid temperature, K
t	time, s
u	system input (manipulated variable)
x	array of the state variables
y	system output (measured variable)

Greeks

α, β, γ	variables defined by equations (22)-(24)
δ	variable defined by equation (27)
$\mathbf{\Lambda}$	matrix of tuning parameters of the Kalman observer
ρ_{Ie}	apparent density of the dried product, kg m^{-3}
ρ_{II}	density of the frozen product, kg m^{-3}

Superscripts

^	observer estimate
.	first time derivative

References

Barresi, A.A., Baldi, G., Parvis, M., Vallan, A., Velardi, S.A., Hammouri H., 2007. Optimization and control of the freeze-drying process of pharmaceutical products. U.S. Patent Application No. 12/296,802 (10/04/2007).

Barresi A.A., Pisano, R., Fissore, D., Rasetto, V., Velardi, S.A.; Vallan, A., Parvis, M., Galan, M., 2009. Monitoring of the primary drying of a lyophilization process in vials. Chemical Engineering and Processing 48, 408-423.

Barresi, A.A., Fissore, D., Marchisio, D.L., 2010a. Process Analytical Technology in industrial freeze-drying. in: Rey, L., May, J.C. (Eds.), Freeze-drying/lyophilization of pharmaceuticals and biological products, 3rd revised Ed., Informa Healthcare, New York, pp. 463-293.

Barresi, A.A., Pisano, R., Rasetto, V., Fissore, D, Marchisio, D.L., 2010b. Model-based monitoring and control of industrial freeze-drying processes: effect of batch non-uniformity. Drying Technology 28, 577-590.

Becerra, V.M., Roberts, P.D., Griffiths, G.W., 2001. Applying the extended Kalman filter to systems described by nonlinear differential-algebraic equations. Control Engineering Practice 9, 267-281.

Chouvenc, P., Vessot, S., Andrieu, J., Vacus, P., 2004. Optimization of the freeze-drying cycle: a new model for pressure rise analysis. Drying Technology 22, 1577-1601.

Corbellini, S., Parvis, M., Vallan, A., 2010. In-process temperature mapping system for industrial freeze-dryers. IEEE Transactions on Instrumentation and Measurement, 59, 1134-1140.

Fissore, D., Velardi, S.A., Barresi, A.A., 2008. In-line control of a freeze-drying process in vial. Drying Technology 26, 685-694.

Fissore, D., Pisano, R., Barresi, A.A., 2010. A model-based framework to get quality-by-design in freeze-drying of pharmaceuticals. Proceedings of Freeze Drying of Pharmaceuticals and Biological Conference, Garmisch-Partenkirchen, September 28 - October 1, 469-470.

Fissore, D., Pisano, R., Barresi, A.A., 2011. On the methods based on the Pressure Rise Test for monitoring a freeze-drying process. Drying Technology 29, 73-90.

Franks, F., 2007. Freeze-drying of pharmaceuticals and biopharmaceuticals. Royal Society of Chemistry, Cambridge.

Gieseler, H., Kessler, W.J., Finson, M., Davis, S.J., Mulhall, P.A., Bons, V., Debo, D.J.,

Pikal, M.J., 2007. Evaluation of Tunable Diode Laser Absorption Spectroscopy for in-process water vapor mass flux measurement during freeze drying. Journal of Pharmaceutical Sciences 96,1776-1793.

Giordano, A., Barresi, A.A., Fissore, D., 2011. On the use of mathematical models to build the design space for the primary drying phase of a pharmaceutical lyophilization process. Journal of Pharmaceutical Sciences 100, 311-324.

Grassini, S., Mombello, D., Neri, A., Parvis, M., Vallan A., 2009. Plasma deposited thermocouple for non-invasive temperature measurement. Proceedings of International Instrumentation and Measurement Technology Conference - I2MTC'09 (IEEE), Singapore, Republic of Singapore, 5-7 May 2009, 732-736. [ISBN: 9781424433520, DOI: 10.1109/IMTC.2009.5168547]

Judd, K., 2003. Nonlinear state estimation, indistinguishable states, and the extended Kalman filter. Physica D 183, 273-281.

Kalman, R.E., 1960. A new approach to linear filtering and prediction. Transaction of the ASME – Journal of Basic Engineering 82, 35- 45.

Kessler, W.J., Davis, S.J., Mulhall, P.A., Finson, M.L., 2006. System for monitoring a drying process. United States Patent No. 0208191 A1.

Kuu, W.Y., Nail, S.L. , Sacha, G., 2009. Rapid determination of vial heat transfer parameters using tunable diode laser absorption spectroscopy (TDLAS) in response to step-changes in pressure set-point during freeze-drying. Journal of Pharmaceutical Sciences 98,1136-1154.

Milton, N., Pikal, M.J., Roy, M.L., Nail, S.L., 1997. Evaluation of manometric temperature measurement as a method of monitoring product temperature during lyophilisation. PDA. Journal of Pharmaceutical Sciences and Technologies 5, 7-16.

Nail, S.L., Gatlin, G.A., 1992. Freeze drying: principles and practice, in: Avis, K.E., Lieberman, H.A., Lachman, L. (Eds.), Pharmaceutical dosage forms: Parenteral medications, vol. 2, Marcell Dekker Inc., New York, pp. 163–233.

Oetjen, G.W., Haseley, P., 2004. Freeze-Drying, 2nd edition. Wiely-VHC, Weinheim

Pikal, M.J., Roy, M.L., Shah, S., 1984. Mass and heat transfer in vial freeze-drying of pharmaceuticals: role of the vial. Journal of Pharmaceutical Sciences 73, 1224-1237.

Velardi, S.A., Barresi, A.A., 2008. Development of simplified models for the freeze-drying process and investigation of the optimal operating conditions. Chemical Engineering Research and Design 87, 9-22.

Velardi, S.A., Rasetto, V., Barresi, A.A., 2008. Dynamic Parameters Estimation Method:

advanced Manometric Temperature Measurement approach for freeze-drying monitoring of pharmaceutical. Industrial and Engineering Chemistry Research 47, 8445-8457.

Velardi, S.A., Hammouri, H., Barresi, A.A., 2009. In line monitoring of the primary drying phase of the freeze-drying process in vial by means of a Kalman filter based observer. Chemical Engineering Research and Design 87, 1409-1419.

Velardi, S.A., Hammouri, H., Barresi, A.A., 2010. Development of a high gain observer for in-line monitoring of sublimation in vial freeze-drying. Drying Technology 28, 256-268.

Appendix A. Observer equations in case of non-constant heating fluid temperature

In case $\frac{du}{dt} \neq 0$ it is necessary to calculate the partial derivative of H respect to variable u, thus obtaining:

$$\frac{\partial H}{\partial u} = \frac{\alpha\left(1-\frac{\gamma}{R_{p,0}}\right)\frac{\partial \beta}{\partial u}}{\left(\frac{\beta}{R_{p,0}}\gamma - \alpha B\right)^2} \tag{A.1}$$

with $\frac{\partial \beta}{\partial u} = R_{p,0}$. In this case, equation (20) is used to calculate $\frac{dx_1}{dt}$, thus obtaining:

$$\frac{dx_1}{dt} = \frac{1}{\delta}\frac{x_3\left(\frac{\gamma}{R_{p,0}}\beta - \alpha B_{R_p}\right)^2\beta}{\left(\gamma - R_{p,0}B_{R_p}\right)\left(\beta\frac{\partial \alpha}{\partial x_1} - \alpha\frac{\partial \beta}{\partial x_1}\right)} + \frac{\partial \beta}{\partial u}\frac{du}{dt}\frac{\alpha\left(1-\frac{\gamma}{R_{p,0}}\right)}{\left(\frac{\gamma}{R_{p,0}} - B\right)\left(\beta\frac{\partial \alpha}{\partial x_1} - \alpha\frac{\partial \beta}{\partial x_1}\right)} \tag{A.2}$$

Equation (A.2) is then used to calculate the Jacobian matrix $\partial \mathbf{f}/\partial \mathbf{x}$, whose components are the followings:

$$\begin{aligned}\frac{\partial f_1}{\partial x_1} = {} & \frac{1}{\delta}\frac{x_3\frac{\partial \beta}{\partial x_1}\left(\frac{\gamma}{R_{p,0}}\beta - \alpha B_{R_p}\right)^2 + 2x_3\beta\left(\frac{\gamma}{R_{p,0}}\beta - \alpha B_{R_p}\right)\left(\frac{\gamma}{R_{p,0}}\frac{\partial \beta}{\partial x_1} - B_{R_p}\frac{\partial \alpha}{\partial x_1}\right)}{\left(\gamma - R_{p,0}B_{R_p}\right)\left(\beta\frac{\partial \alpha}{\partial x_1} - \alpha\frac{\partial \beta}{\partial x_1}\right)} + \\ & + \frac{1}{\delta}\frac{x_3\beta\left(\frac{\gamma}{R_{p,0}}\beta - \alpha B_{R_p}\right)^2}{\left(\gamma - R_{p,0}B_{R_p}\right)}\frac{\alpha\frac{\partial^2 \beta}{\partial x_1^{\,2}} - \beta\frac{\partial^2 \alpha}{\partial x_1^{\,2}}}{\left(\beta\frac{\partial \alpha}{\partial x_1} - \alpha\frac{\partial \beta}{\partial x_1}\right)^2} + \\ & + \frac{\partial \beta}{\partial u}\frac{du}{dt}\left[\frac{\left(1-\frac{\gamma}{R_{p,0}}\right)\frac{\partial \alpha}{\partial x_1}}{\left(\frac{\gamma}{R_{p,0}} - B_{R_p}\right)\left(\beta\frac{\partial \alpha}{\partial x_1} - \alpha\frac{\partial \beta}{\partial x_1}\right)} + \frac{\alpha\left(1-\frac{\gamma}{R_{p,0}}\right)}{\left(\frac{\gamma}{R_{p,0}} - B_{R_p}\right)}\frac{\alpha\frac{\partial^2 \beta}{\partial x_1^{\,2}} - \beta\frac{\partial^2 \alpha}{\partial x_1^{\,2}}}{\left(\beta\frac{\partial \alpha}{\partial x_1} - \alpha\frac{\partial \beta}{\partial x_1}\right)^2}\right]\end{aligned} \tag{A.3}$$

$$\frac{\partial f_1}{\partial x_2}=\frac{x_3}{\delta\left(\alpha\dfrac{\partial\beta}{\partial x_1}-\beta\dfrac{\partial\alpha}{\partial x_1}\right)}\frac{\partial\gamma}{\partial x_2}\frac{\dfrac{2\beta^2}{R_{p,0}}\left(\dfrac{\gamma}{R_{p,0}}\beta-\alpha B_{R_p}\right)\left(\gamma-R_{p,0}B_{R_p}\right)-\beta\left(\dfrac{\gamma}{R_{p,0}}\beta-\alpha B_{R_p}\right)^2}{\left(\gamma-R_{p,0}B_{R_p}\right)^2}+$$
$$+\frac{\partial\beta}{\partial u}\frac{du}{dt}\left[\frac{\partial\gamma}{\partial x_2}\frac{\alpha\left(\dfrac{\gamma}{R_{p,0}}-1\right)}{\left(\dfrac{\gamma}{R_{p,0}}-B_{R_p}\right)^2R_{p,0}\left(\beta\dfrac{\partial\alpha}{\partial x_1}-\alpha\dfrac{\partial\beta}{\partial x_1}\right)}-\frac{\partial\gamma}{\partial x_2}\frac{\dfrac{\alpha}{R_{p,0}}}{\left(\dfrac{\gamma}{R_{p,0}}-B_{R_p}\right)\left(\beta\dfrac{\partial\alpha}{\partial x_1}-\alpha\dfrac{\partial\beta}{\partial x_1}\right)}\right] \tag{A.4}$$

$$\frac{\partial f_1}{\partial x_3}=\frac{1}{\delta}\frac{\beta\left(\dfrac{\gamma}{R_{p,0}}\beta-\alpha B_{R_p}\right)^2-2x_3\beta\left(\dfrac{\gamma}{R_{p,0}}\beta-\alpha B_{R_p}\right)\dfrac{\partial\alpha}{\partial x_3}B_{R_p}}{\left(\gamma-R_{p,0}B_{R_p}\right)\left(\beta\dfrac{\partial\alpha}{\partial x_1}-\alpha\dfrac{\partial\beta}{\partial x_1}\right)}+$$
$$+\frac{1}{\delta}\frac{x_3\beta\left(\dfrac{\gamma}{R_{p,0}}\beta-\alpha B_{R_p}\right)^2}{\left(\gamma-R_{p,0}B_{R_p}\right)}\frac{\left(\dfrac{\partial\beta}{\partial x_1}\dfrac{\partial\alpha}{\partial x_3}-\beta\dfrac{\partial^2\alpha}{\partial x_1\partial x_3}\right)}{\left(\beta\dfrac{\partial\alpha}{\partial x_1}-\alpha\dfrac{\partial\beta}{\partial x_1}\right)^2}+ \tag{A.5}$$
$$+\frac{\partial\beta}{\partial u}\frac{du}{dt}\left[\frac{\dfrac{\partial\alpha}{\partial x_3}\left(1-\dfrac{\gamma}{R_{p,0}}\right)}{\left(\dfrac{\gamma}{R_{p,0}}-B_{R_p}\right)\left(\beta\dfrac{\partial\alpha}{\partial x_1}-\alpha\dfrac{\partial\beta}{\partial x_1}\right)}+\frac{\alpha\left(1-\dfrac{\gamma}{R_{p,0}}\right)}{\left(\dfrac{\gamma}{R_{p,0}}-B_{R_p}\right)}\frac{\left(\dfrac{\partial\beta}{\partial x_1}\dfrac{\partial\alpha}{\partial x_3}-\beta\dfrac{\partial^2\alpha}{\partial x_1\partial x_3}\right)}{\left(\beta\dfrac{\partial\alpha}{\partial x_1}-\alpha\dfrac{\partial\beta}{\partial x_1}\right)^2}\right]$$

List of Tables

Table 1. Values of $\hat{K}_v(t=0)$ and $\hat{A}_{R_p}(t=0)$ used for observer validation with simulated data.

Table 2. Values of $\hat{K}_v(t=0)$ and $\hat{A}_{R_p}(t=0)$ used to validate the observer with experimental data.

List of Figures

Figure 1. Comparison between estimated (lines) and true values (symbols) of product temperature (top graphs; ○: T_B, ●: T_i, —: T_i), moving front position (middle graphs) and model parameters (bottom graphs; ● and —: R_p, ○ and – – –: K_v) for two case studies (case 1: K_v = 30.0 J $s^{-1}m^{-2}K^{-1}$, A_{R_p} = $1.0 \cdot 10^9$ s^{-1}; case 2: K_v = 10.0 J $s^{-1}m^{-2}K^{-1}$, A_{R_p} = $2.0 \cdot 10^8$ s^{-1}; $R_{p,0}$ = $1.1 \cdot 10^4$ m s^{-1}, B_{R_p} = $2.0 \cdot 10^3$ m^{-1}, L = 7.6 mm, T_{fluid} = -10°C, p_c = 8 Pa).

Figure 2. Comparison between true (—: T_B, – – –: T_i) and estimated values (symbols: T_i; □: case 1, ○: case 2, Δ: case 3, ●: case 4) of product temperature (graph a), moving front position (graph b), heat transfer coefficient (graph c), and product resistance to vapor flow (graph d).

Figure 3. Range of values of errors on initial estimations of K_v and A_{R_p} that ensures the convergence of the observer: symbols (■: values of e_{K_v} and $e_{A_{R_p}}$ for which the convergence of the observer is obtained; □: values of e_{K_v} and $e_{A_{R_p}}$ for which the convergence of the observer is not obtained).

Figure 4. Comparison between estimated (lines) and true values (symbols) of product temperature at the interface of sublimation (graph a), moving front position (graph b), heat transfer coefficient (graph c), and product resistance to vapor flow (graph d) (K_v = 16.2 J $s^{-1}m^{-2}K^{-1}$, $R_{p,0}$ = 33969 m s^{-1}, A_{R_p} = $1.06 \cdot 10^8$ s^{-1} and B_{R_p} = 0 m^{-1}, L = 3.4 mm, T_{fluid} = -10°C, p_c = 8 Pa).

Figure 5. Comparison between experimentally measured values (symbols) of product temperature and the values estimated by the observer using the initial estimations of model parameters given in Table 2 (lines; —: T_i, – – –: T_B).

Figure 6. Range of values of errors on initial estimations of K_v and A_{R_p} that ensures the convergence of the observer (■: values of e_{K_v} and $e_{A_{R_p}}$ for which the convergence

of the observer is obtained; □: values of e_{K_v} and $e_{A_{R_p}}$ for which the convergence of the observer is not obtained).

Table 1

	$\hat{K}_v\left(t=0\right)$, J s^{-1} m^{-2} K^{-1}	e_{K_v}	$\hat{A}_{R_p}\left(t=0\right)$, s^{-1}	e_{R_p}
case 1	18.81	+10 %	$4.305 \cdot 10^8$	+5 %
case 2	15.39	-10 %	$3.895 \cdot 10^8$	-5 %
case 3	20.52	+20 %	$4.510 \cdot 10^8$	+10 %
case 4	15.39	-10 %	$4.305 \cdot 10^8$	+5 %

Table 2

	$\hat{K}_v\left(t=0\right)$, J s^{-1} m^{-2} K^{-1}	e_{K_v}	$\hat{A}_{R_p}\left(t=0\right)$, s^{-1}	e_{R_p}
case 1	13.68	-20 %	$2.52\cdot10^{8}$	-5 %
case 2	20.52	+20 %	$2.52\cdot10^{8}$	-5 %
case 3	13.68	-20 %	$2.78\cdot10^{8}$	+5 %
case 4	20.52	+20 %	$2.78\cdot10^{8}$	+5 %

Figure 1

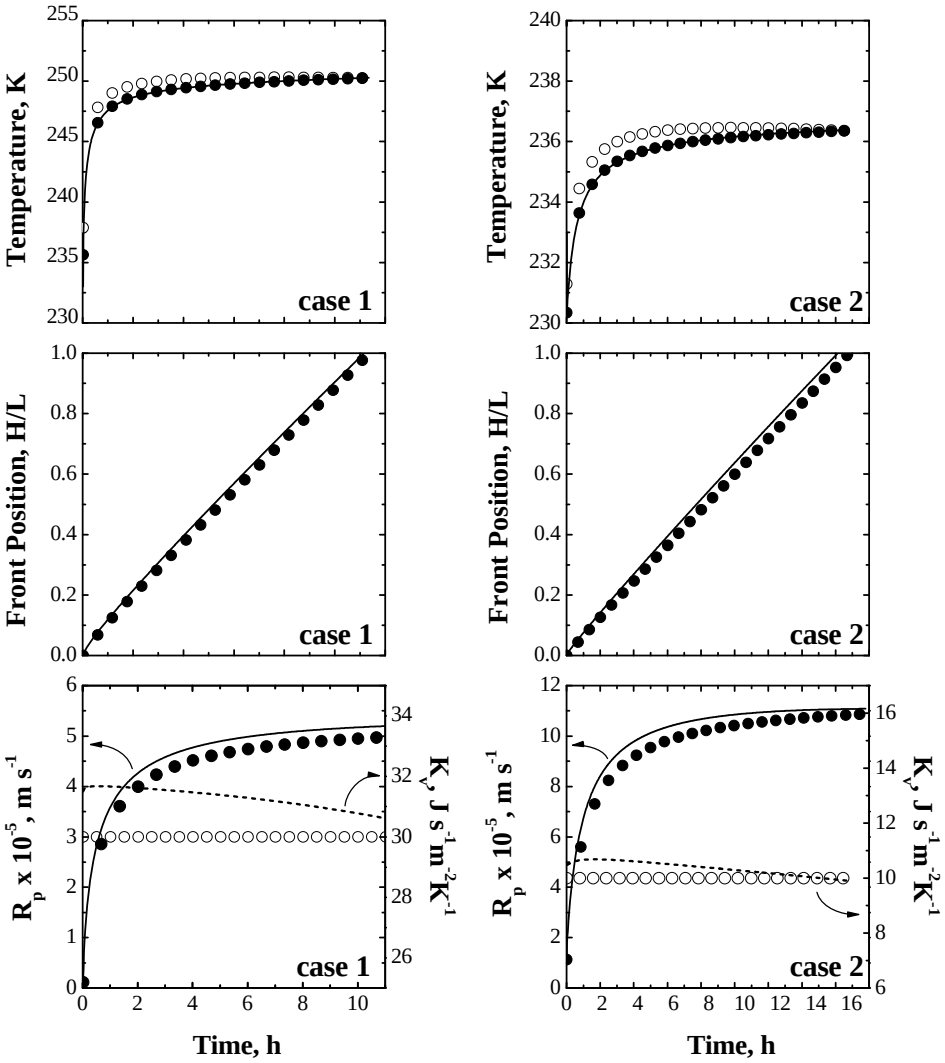
Temperature, K
case 1
Front Position, H/L
case 1
R_p x 10^{-5}, m s^{-1}
K_v, J s^{-1} m^{-2} K^{-1}
case 1
Time, h
Temperature, K
case 2
Front Position, H/L
case 2
R_p x 10^{-5}, m s^{-1}
K_v, J s^{-1} m^{-2} K^{-1}
case 2
Time, h

Figure 2

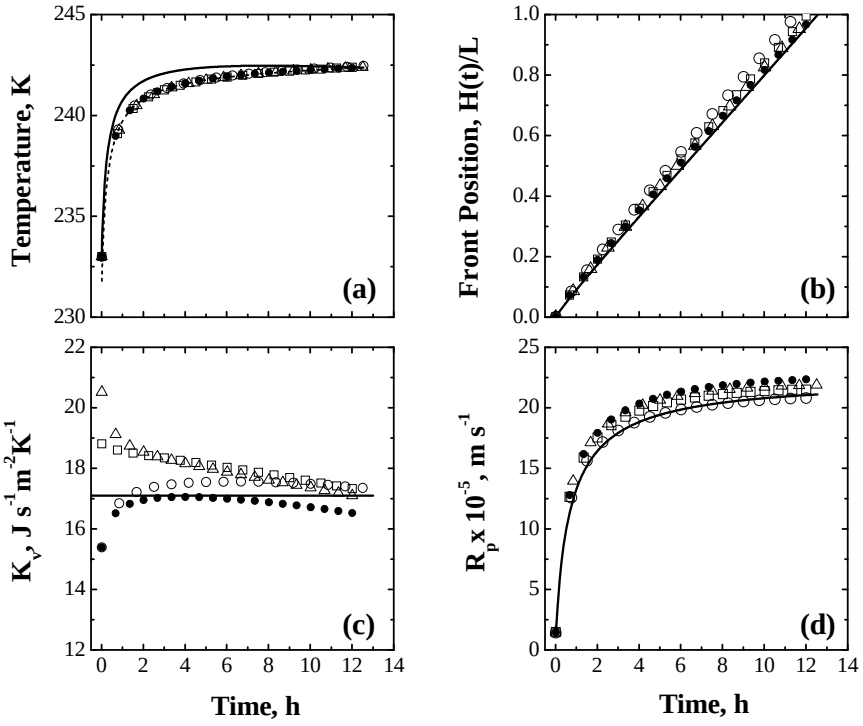
Temperature, K
245
240
235
230
(a)
Front Position, H(t)/L
1.0
0.8
0.6
0.4
0.2
0.0
(b)
K_v, J s^{-1}m^{-2}K^{-1}
22
20
18
16
14
12
(c)
R_p x 10^{-5}, m s^{-1}
25
20
15
10
5
0
(d)
0 2 4 6 8 10 12 14
Time, h
Time, h

Figure 3

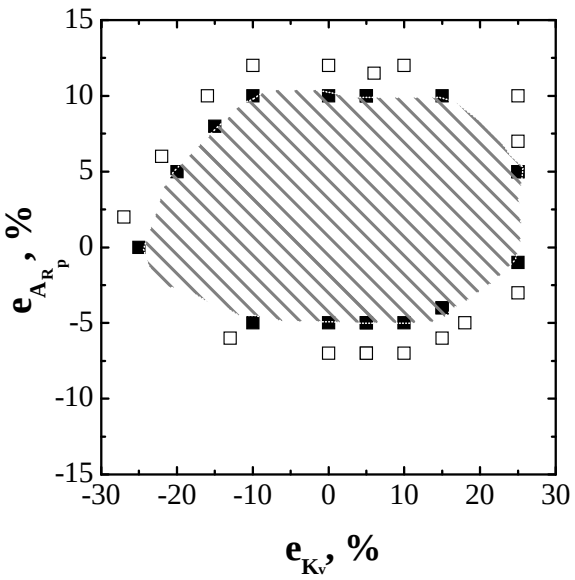

Figure 4

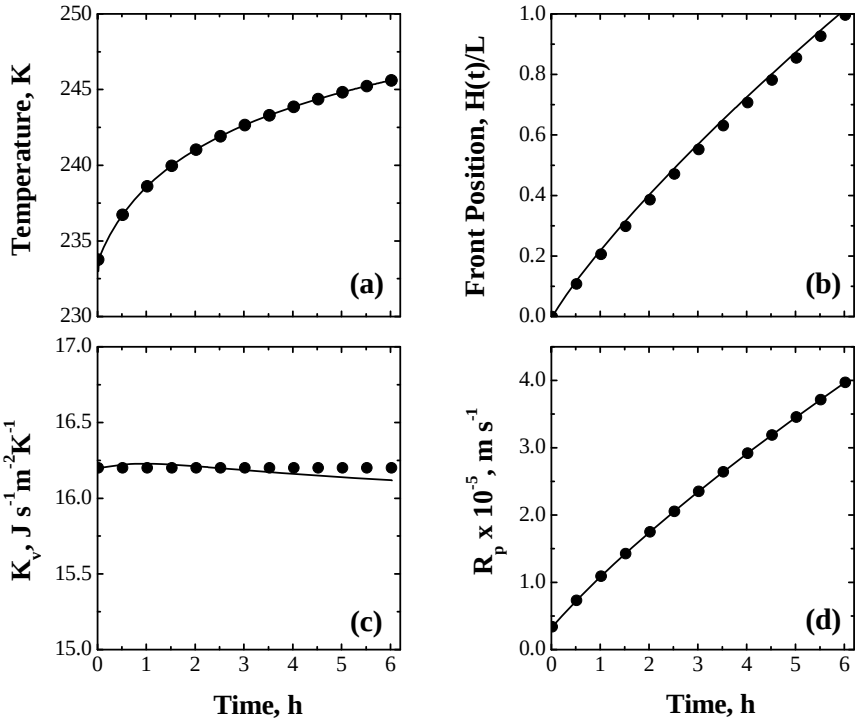
Temperature, K
250
245
240
235
230
(a)
Front Position, H(t)/L
1.0
0.8
0.6
0.4
0.2
0.0
(b)
K_v, J s^{-1}m^{-2}K^{-1}
17.0
16.5
16.0
15.5
15.0
(c)
R_p x 10^{-5}, m s^{-1}
4.0
3.0
2.0
1.0
0.0
(d)
0 1 2 3 4 5 6
Time, h
Time, h

Figure 5

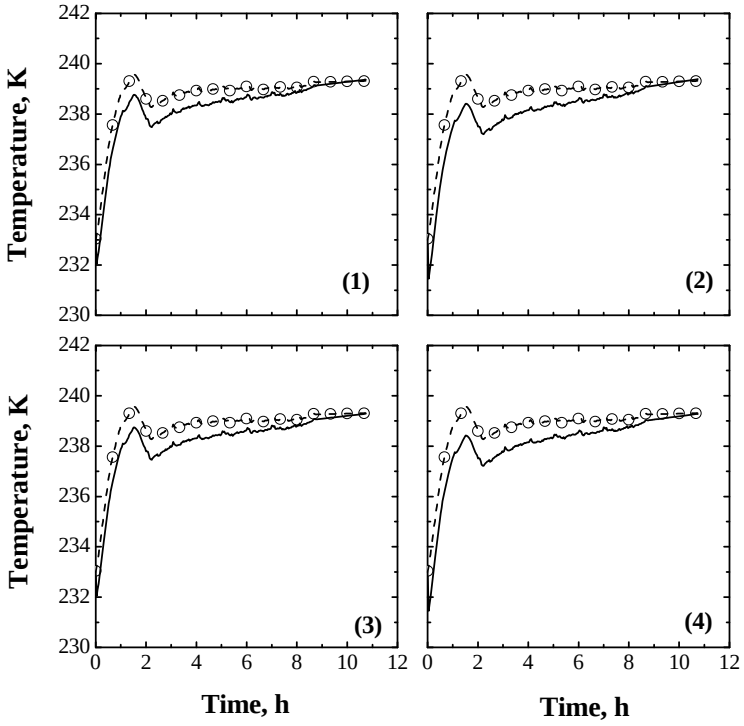
Temperature, K
Time, h
(1)
(2)
(3)
(4)
242
240
238
236
234
232
230
0
2
4
6
8
10
12

Figure 6

